Finite Element Modeling for Vibration of Initially Stressed Non-local Euler-Bernoulli Beams

Çiğdem Dinçkal

Çankaya University, Faculty of Engineering, Department of Civil Engineering, Ankara, Türkiye,
+90 312 2331405,
cdinckal@cankaya.edu.tr

Abstract

This paper is concerned with a precise finite element model for vibration analysis of initially stressed micro/nano beams based on nonlocal Euler-Bernoulli and Eringen's nonlocal elasticity theory. For this purpose analytical solutions for the exact dynamic shape functions has been derived by also use of Hamiltonian's principle for the governing equations. The solution is applicable to various initial stresses such as tensile and compressive and scaling effect. The exact dynamic shape functions have been constructed to obtain analytic expressions for the exact dynamic element stiffness matrix components. Numerical results are displayed to indicate the effects of initial stresses and scaling effect parameters on the vibration characteristics of initially stressed clamped nonlocal Euler-Bernoulli beams. For the first time in literature, this study presents such an element formulation that it provides adequate and accurate representation of the vibration behavior of initially stressed micro/nano beams based on nonlocal Euler-Bernoulli beam theory.

Keywords — Exact Dynamic Shape Functions, Exact Dynamic Stiffness Matrix, Finite Element Method, Initially Stressed Nonlocal *Euler-Bernoulli* Beams, Nonlocal Elasticity

1 Introduction

Nano/micro structures such as nanobeams, nanotubes hold great promises for many technologically critical applications such as NEMS/MEMS devices, nanowires [1, 2, 3].

During the fabrication of micro/nano structures, the axial residual stress effects are usually indispensable. Initial stresses are prevailing in the nanoscale systems by the reason of a high proportion of surface atoms. Initial stresses are available in unstretched nanostructures upon thermal equilibration in molecular dynamics simulation of nanostructures. Furthermore, in the analysis of these structures, Wang and Hu [4] showed that classical beam theories are inadequate to grasp the small scale effect in the mechanical properties of micro/nano structures. In other words, these theo-ries are not sufficient to predict the decrease in phase velocities of wave propagation in a single–walled carbon nanotube when the wave number is so large. Eringen [5, 6, 7] proposed the theory of nonlocal continuum mechanics in order to take account of the small scale effect. This theory is used to modify the beam theory for analysis of micro/nano beams. Some researchers have employed the nonlocal elasticity theory for vibration, the bending, and buckling analyses in micro-or nanoelectromechanical devices [8, 9, 10, 11, 12, 13, 14]. In literature, vibration of beams based on Timoshenko beam theory has been studied [15, 16, 17, 18, 19, 20]. Though, a few studies have been elaborated on the analysis of vibration behavior of the initially stressed micro/nano beams [21, 22]. These studies employed only Timoshenko beam theory. Neither of them uses nonlocal Euler-Bernoulli beam theory.

In the literature, some studies used or derived finite element formulations [23, 24, 25]. They have focalized the vibration analysis from the point of non-local, small-scale effects in Euler-Bernoulli or Timoshenko beam theory by employing number of elements to converge exact (also analytical) solutions. Neither of them has employed nor derived an exact element which leads to analytical solutions for the vibration problem of nanostructures. Instead, they have increased the number of employed elements to minimize error due to the deviation from exact results.

In these premises, the present work aims to analyze the vibration behavior of the initially stressed (compressive or tensile) micro/nano beam based on Eringen's nonlocal elasticity and nonlocal Euler-Bernoulli beam theory by improving finite element method with only one element per member. In the 1960s, finite element method introduced commonly, and formulations of which are based on cubic Hermitian functions [26]. It has been a very popular tool for some researchers [27, 28, 29, 30] to elaborate on the effects of vibration of many structures.

In this paper, Hamiltonian's principle is used in the derivation of both exact dynamic shape functions and stiffness matrix for the clamped end boundary conditions.

Owing to employ exact shape functions and dynamic stiffness terms, the proposed solution exactly satisfies equilibrium equations at both the element nodes and within the element. This is one of the advantages of the derived element, and it only needs one element per member to attain exact results. Explicit forms of both exact dynamic shape functions and stiffness terms are also given in this paper. Numerical results for free vibration of initially stressed nonlocal Euler-Bernoulli beams are also presented to indicate the advantages of the proposed solutions.

2 Materials and Method
2.1 Equations of nonlocal Euler-Bernoulli beam
To the Euler-Bernoulli beam theory [4, 5, 7, 18], the strain-displacement relation is

$$\varepsilon_{xx} = -z \frac{d^2 w}{dx^2} \ (2.1)$$

here, x is the longitudinal coordinate which is measured from the left end of the beam, z is the coordinate which is measured from the midplane of the beam, w the transverse displacement and ε_{xx} is the normal strain. The virtual strain energy δU is represented by

$$\delta U = \iint_0^L {}_A \sigma_{xx} \, \delta \, \varepsilon_{xx} dA dx \ (2.2)$$

here, σ_{xx} is the normal stress, L is the length of the beam and A is the cross-sectional area. By putting Eq. (2.1) into Eq. (2.2), the strain energy can be stated as

$$\delta U = - \int_0^L M \frac{d^2 \delta w}{dx^2} dx \ (2.3)$$

where the bending moment M is expressed as

$$M = \int_A \sigma_{xx} z dA \ (2.4)$$

When a compressive initial stress σ_o exists, the virtual potential energy δV of the initial stress is represented by

$$\delta V = - \int_0^L \sigma_o A \frac{d\delta w}{dx} \frac{dw}{dx} dx \ (2.5)$$

A negative value of σ_o represents an initial tensile stress. By considering that motion is free harmonic, the virtual kinetic energy δT is given by

$$\delta T = \int_0^L \rho A w \omega^2 \, \delta w dx \ (2.6)$$

here, ω is the circular frequency and ρ is the mass density of the beam material. To Hamiltonian's principle, one can obtain

$$\delta(U + V - T) = 0$$

$$\delta(U + V - T) = \int_0^L \left(\begin{matrix} -M \frac{d^2 \delta w}{dx^2} - \sigma_o A \frac{d\delta w}{dx} \frac{dw}{dx} \\ -\rho A \omega^2 w \delta w \end{matrix} \right) dx \ (2.7)$$

By arranging this integral by integration by parts, the following is obtained

$$\int_0^L \left(\frac{d^2 M}{dx^2} - \sigma_o A \frac{d^2 w}{dx^2} + \rho A \omega^2 w \right) \delta w dx$$

$$+ \left[M \frac{d\delta w}{dx} - \frac{dM}{dx} \delta w + \sigma_o A \frac{dw}{dx} \delta w \right]_0^L = 0 \ (2.8)$$

Since δw is arbitrary in $0 < x < L$, the following governing equation of motion may be obtained

$$\frac{d^2 M}{dx^2} = \sigma_o A \frac{d^2 w}{dx^2} - \rho A \omega^2 w \ (2.9)$$

On account of Eq. (2.8), nonlocal Euler-Bernoulli beam theory's boundary conditions are

$$w = 0 \quad \text{or} - \frac{dM}{dx} + \sigma_o A \frac{dw}{dx} = 0 \ (2.10)$$

$$\frac{dw}{dx} = 0 \text{ or } M = 0 \ (2.11)$$

Either one of these conditions may be specified. In one dimensional case, for an elastic material, Eringen's complicated nonlocal constitutive relation may be rearranged to [7]

$$\sigma_{xx} - (e_0 a)^2 \frac{d^2 \sigma_{xx}}{dx^2} = E \varepsilon_{xx} \ (2.12)$$

Here, E is the Young's modulus and e_0a is the scale coefficient in which a is the internal characteristic length (e.g. lattice parameter, molecular diameter and granular size) and e_0 is a constant which is to be determined experimentally or by calibrating with atomistic modeling. By multiplying Eq. (2.12) by zdA and integrating the results over the area A gives

$$M - (e_0a)^2 \frac{d^2M}{dx^2} = -EI\frac{d^2w}{dx^2} \text{ (2.13)}$$

here I is the moment of inertia. By putting the Eq. (2.9) into Eq. (2.13), one can obtain

$$M = -EI\frac{d^2w}{dx^2} + (e_0a)^2\left(\sigma_oA\frac{d^2w}{dx^2} - \rho A\omega^2w\right) \text{ (2.14)}$$

Therefore, the governing equation for the vibration of nonlocal Euler-Bernoulli beams becomes

$$(EI - (e_0a)^2\sigma_oA)\frac{d^4w}{dx^4} + ((e_0a)^2\rho A\omega^2 +$$

$$\sigma_oA)\frac{d^2w}{dx^2} - \rho A\omega^2 w = 0 \quad \text{(2.15)}$$

To simplify the equations, the following nondimensional terms are expressed as follows:

$$\bar{x} = \frac{x}{L} \text{ and } \bar{w} = \frac{w}{L} \text{ (2.16)}$$

Frequency parameter is represented by

$$\lambda = \sqrt{\omega^2\frac{\rho AL^4}{EI}} \text{ (2.17)}$$

Scaling effect parameter is stated as
$$\alpha = \frac{e_0a}{L} \text{ (2.18)}$$

Initial stress parameter is
$$\Lambda = \sigma_o\frac{AL^2}{EI} \text{ (2.19)}$$

By use of the parameters given in Eqs. (2.16)-(2.19), Eq. (2.15) may be rewritten as

$$A_1\frac{d^4\bar{w}}{dx^4} + A_2\frac{d^2\bar{w}}{dx^2} + A_3\bar{w} = 0 \text{ (2.20)}$$

where the coefficients A_i, i=1, 2, 3 are expressed in terms of scaling effect and initial stress parameters and given by

$$A_1 = 1 - \alpha^2\Lambda, \; A_2 = \alpha^2\lambda^2 + \Lambda, \quad A_3 = -\lambda^2 \text{ (2.21)}$$

In view of Eqs. (2.10) and (2.11), for simply supported end, two boundary conditions related with the nonlocal Euler-Bernoulli beam theory at each end of the beam are expressed as

$$w = 0$$
$$M = -EI\frac{d^2w}{dx^2} + (e_0a)^2\left(\sigma_oA\frac{d^2w}{dx^2} - \rho A\omega^2w\right) \text{ (2.22)}$$

For a free end, the boundary conditions are

$$M = -EI\frac{d^2w}{dx^2} + (e_0a)^2\left(\sigma_oA\frac{d^2w}{dx^2} - \rho A\omega^2w\right) = 0$$
$$-\frac{dM}{dx} + \sigma_oA\frac{dw}{dx} = 0 \text{ (2.23)}$$

The boundary conditions for clamped end
$$w = 0 \text{ and } \frac{dw}{dx} = 0 \text{ (2.24)}$$

Clamped end type boundary conditions are taken into account in the present paper.

2.2 Finite Element Method

Some steps about the execution of finite element analysis to the problem described briefly in this section. Firstly Eq. (2.20) may be rewritten as
$$\frac{d^4\bar{w}}{dx^4} + B_1\frac{d^2\bar{w}}{dx^2} + B_2\bar{w} = 0 \text{ (2.25)}$$

where

$$B_1 = \frac{A_2}{A_1}, \; B_2 = \frac{A_3}{A_1} \text{ (2.26)}$$

The expression in Eq. (2.26) yield the followings respectively

$$B_1 = \frac{\alpha^2\lambda^2+\Lambda}{1-\alpha^2\Lambda}, \; B_2 = \frac{-\lambda^2}{1-\alpha^2\Lambda} \text{ (2.27)}$$

In Eq. (2.25), the roots are

$$R_1 = \eta, \quad R_2 = -\eta, \; R_3 = \xi, \quad R_4 = -\xi \text{ (2.28)}$$

where

$$\eta = \frac{\sqrt{-B_1 - \sqrt{B_1^2 - 4B_2}}}{\sqrt{2}}, \quad \xi$$
$$= \frac{\sqrt{-B_1 + \sqrt{B_1^2 - 4B_2}}}{\sqrt{2}}$$

(2.29)

It should be noted that there exists three possible sets of solutions: These possible sets are; case 1 (if $B_1 < 2\sqrt{B_2}$), case 2 (if $B_1 = 2\sqrt{B_2}$)) and case 3 (if $B_1 > 2\sqrt{B_2}$)). Each sub-case is analyzed individually such that the exact shape functions have been derived for each case.

<u>Case 1 if</u> $B_1 < 2\sqrt{B_2}$:

The complementary solution for Eq. (2.25) becomes:

$$y(x) = c_1\cosh[\eta x]\cos[\xi x] + c_2\cosh[\eta x]\sin[\xi x]$$

$$+c_3\sinh[\eta x]\cos[\xi x] + c_4\sinh[\eta x]\sin[\xi x] \text{ (2.30)}$$

The constants $c_1 - c_4$ can be found by considering the following boundary conditions:

$$y(0) = v_1 \; , \; \frac{dy}{dx}(0) = \theta_1,$$

$$y(L) = v_2 \ , \frac{dy}{dx}(L) = \theta_2 \ (2.31)$$

Then,

$$\begin{Bmatrix} v_1 \\ \theta_1 \\ v_2 \\ \theta_2 \end{Bmatrix} = G \begin{Bmatrix} c_1 \\ c_2 \\ c_3 \\ c_4 \end{Bmatrix} \ (2.32)$$

The matrix G can be formed by putting the boundary conditions into Eq. (2.30). Finally, Eq. (2.32) is solved to find $c_1 - c_4$ and then, this result is substituted back into Eq. (2.30) to attain the following:

$$y(x) = \lfloor N_1 \quad N_2 \quad N_3 \quad N_4 \rfloor \begin{Bmatrix} v_1 \\ \theta_1 \\ v_2 \\ \theta_2 \end{Bmatrix} \ (2.33)$$

$N_1 - N_4$ are the exact dynamic shape functions directly obtained from the solution of Eq. (2.25). The related equation in Eq. (2.25) is satisfied in Eq. (2.33). It is also checked that $N_1 - N_4$ converges to Hermitian (cubic) polynomials at the limit (such as, α and $\Lambda \to 0$).

Explicit form of the shape functions are presented in Appendix A.

Case 2 if $B_1 = 2\sqrt{B_2}$:

Eq. (2.25) roots are

$$R_1 = \beta i \ , \ R_2 = -\beta i, \ R_3 = \gamma i, \ R_4 = -\gamma i \quad (2.34)$$

where

$$\beta = \gamma = \sqrt{\frac{B_1}{2}}$$

Eq. (2.25) complementary solution in case 2 takes the following form:

$$y(x) = c_1 \cos[\beta x] + c_2 \, x \cos[\beta x] + c_3 \sin[\beta x]$$
$$+c_4 \, x \sin[\beta x] \ (2.35)$$

To attain the constants; $c_1 - c_4$ given in Eq. (2.35), Eqs. (2.31)-(2.33) are applied. As a result the shape functions for case 2 are derived and explicit expressions of them are presented in Appendix B.

Case 3 if $B_1 > 2\sqrt{B_2}$:

The roots of Eq. (2.25) are

$$E_1 = \beta i \ , \ E_2 = -\beta i, \ E_3 = \gamma i, \ E_4 = -\gamma i \ (2.36)$$

Where

$$\beta = \frac{\sqrt{B_1 - \sqrt{B_1{}^2 - 4B_2}}}{\sqrt{2}}, \qquad \gamma = \frac{\sqrt{B_1 + \sqrt{B_1{}^2 - 4B_2}}}{\sqrt{2}} \quad (2.37)$$

Then, Eq. (2.25) complementary solution in case 3 becomes

$$y(x) = c_1 \cos[\beta x] \ + c_2 \cos[\gamma x] + c_3 \sin[\beta x]$$
$$+c_4 \sin[\gamma x] \ (2.38)$$

To find the constants; $c_1 - c_4$ given in Eq. (2.38), Eqs. (2.31)-(2.33) are applied. As a result case 3 shape functions are derived and explicit expressions of them are presented in Appendix C.

Moreover, the shape functions derived for each case, converge to the cubic Hermitian polynomials in the limits (i.e. α and $\Lambda \to 0$) by letting $\gamma \ \xi, \eta$ and β approach zero in equations given in Appendix A, B and C. Therefore cubic Hermitian polynomials can be obtained as follows:

$$N_1 = \frac{(L-x)^2(L+2x)}{L^3} \ (2.39)$$

$$N_2 = \frac{(L-x)^2 x}{L^2} \ (2.40)$$

$$N_3 = \frac{(3L-2x)x^2}{L^3} \ (2.41)$$

$$N_4 = \frac{x^2(-L+x)}{L^2} \ (2.42)$$

These expressions lead to accurate computations in that one can successively modify equations given in Appendix A, B, C to Eqs. (2.39), (2.40), (2.41), (2.42) by allowing both B_1 and B_2 to approach zero.

Subsequently, the following equation computes the dynamic stiffness matrix components:

$$K_{ij} = \int_0^L \frac{d^2 N_i}{dx^2} \frac{d^2 N_j}{dx^2} dx - B_1 \int_0^L \frac{dN_i}{dx} \frac{dN_j}{dx} dx$$
$$+B_2 \int_0^L N_i N_j dx \ (2.43)$$

In Eq. (2.43), the first integral gives material stiffness terms, the second integrals are associated with element attributed to scaling effect parameter, initial stress parameter and also frequency. The term N_i represents i^{th} shape function and all of the above integrals are practiced over the element length L. The second integral has a destabilizing effect on the stiffness terms. Dynamic stiffness terms can be attained by solving the integral in Eq. (2.43). The explicit expressions of the dynamic stiffness terms for each case are presented in Appendix D, E and F respectively.

2.2.1 Mass matrix

Mass matrix is attained by computation of the third integral in Eq. (2.43). The 4×4 mass matrix **m** with

regards to shape functions of a uniform segment with mass per unit length is obtained by the calculation of the following integral [27, 28, 29].

$$\mathbf{m} = B \int \mathbf{N}^T N dx \quad (2.44)$$

When computing the integral β, γ, η and ξ are set to zero which is the case of employing Hermitian interpolation functions, then the 4×4 becomes:

$$\mathbf{m} = \frac{B_2}{420} \begin{bmatrix} 156 & 22L & 54 & -13L \\ 22L & 4L^2 & 13L & -3L^2 \\ 54 & 13L & 156 & -22L \\ -13L & -3L^2 & -22L & 4L^2 \end{bmatrix} \quad (2.45)$$

2.2.2 Geometric stiffness matrix

Geometric stiffness matrix is constructed by computation of the second integral in Eq. (2.43). The 4×4 geometric stiffness matrix $\boldsymbol{K_G}$ is associated with the terms of shape functions for the combination of scaling effect, initial stress and frequency parameter. This matrix terms can be attained by the calculation of the following integral [27, 28, 29].

$$\boldsymbol{K_G} = B_1 \int \frac{d\mathbf{N}^T}{dx}\frac{dN}{dx} dx \quad (2.46)$$

The terms in Eq. (2.47) have also been attained in closed form when β, γ, η and ξ are set to zero which is the case of employing Hermitian interpolation functions. The 4×4 matrix takes the following form:

$$\boldsymbol{K_G} = \frac{B_1}{30L} \begin{bmatrix} 36 & 3L & -36 & 3L \\ 3L & 4L^2 & -3L & -L^2 \\ -36 & -3L & 36 & -3L \\ 3L & -L^2 & -3L & 4L^2 \end{bmatrix} \quad (2.47)$$

Eq. (2.47) and Eq. (2.45) are simply the consequences of Eq. (2.46) and Eq. (2.44), respectively, for

$\beta=\gamma=\eta=\xi=0$. When only $\Lambda = 0$ is assumed, the solution is for nonlocal Euler-Bernoulli beam theory without initial stress.

2.2.3 Stiffness matrix

When β, γ, η, ξ are set to zero which is the case of employing Hermitian interpolation functions, the integral in Eq. (2.43) has been calculated for each stiffness terms. Therefore, following 4×4 consistent stiffness matrix is obtained.

$$\boldsymbol{K} = \frac{1-\alpha^2\Lambda}{L^3} \begin{bmatrix} 12 & 6L & -12 & 6L \\ 6L & 4L^2 & -6L & 2L^2 \\ -12 & -6L & 12 & -6L \\ 6L & 2L^2 & -6L & 4L^2 \end{bmatrix} \quad (2.48)$$

3 Numerical Results

Numerical analysis associated with vibration of initial stressed clamped micro/nano beams based on nonlocal Euler-Bernoulli beam theory is given in this section. Vibration frequencies are computed with the constituted element for each case. It is important to note that these frequencies λ makes the determinant of stiffness matrix zero. For this reason an eigenvalue analysis is performed in such a way that

$\left((K + K_G) - \lambda^2 M\right)\Phi = 0$ where K, K_G and M are the assembled stiffness, geometric stiffness and mass matrices, respectively and Φ are the eigenvalues (mode shapes) which express the corresponding shapes of the vibrating system. The final eigenvalue matrix size is 4×4 for clamped end type boundary conditions. It is important to note that various boundary conditions give different shape functions. This study has focalized clamped end type boundary condition. The proposed element is put into a finite element library executed in Mathematica [31]. Consider a clamped end micro/nano beam with diameter: 0.678 nm and length L:6.78 nm with different scaling effect parameter (α): 0, 0.1, 0.2, 0.3, 0.4, 0.5 and various initial stresses such as Λ:-40,-30,-20,-10,0,2,3,6,8,10,12,14,16,18 Pa. It should be noted that a negative value of Λ refers an initial tensile stress.

In case of tensile initial stresses, the frequency parameters for clamped micro/nano beam with various scaling effect parameters are calculated for all cases and presented in Table 1.

Table 1. Frequency parameter for clamped micro/nano beam with various scaling effect and tensile initial stresses for all cases

Initial Stress	Case	Alpha(α)

		0	0.1	0. 2	0. 3	0. 4	0. 5
	$B_1 < \sqrt{2B_2}$	18.809	18.301	18.29	18.256	15.809	12.645
-40	$B_1 > \sqrt{2B_2}$	5.3538	4.3145	2.2804	3.0337	2.3791	2.6633
	$B_1 = \sqrt{2B_2}$	6.3246	6.2932	6.2017	6.0578	5.8722	5.6568
	$B_1 < \sqrt{2B_2}$	15.675	15.3302	15.818	14.905	13.691	10.952
-30	$B_1 > \sqrt{2B_2}$	5.1602	3.46759	2.0976	2.7213	1.9722	2.2549
	$B_1 = \sqrt{2B_2}$	5.4772	5.4500	5.3709	5.2462	5.0855	4.899
	$B_1 < \sqrt{2B_2}$	14.883	13.8988	16.634	10.539	11.178	8.9415
-20	$B_1 > \sqrt{2B_2}$	2.7271	1.69128	1.8974	1.5067	1.6259	1.5935
	$B_1 = \sqrt{2B_2}$	4.4721	4.44994	4.3853	4.2835	4.1523	4
	$B_1 < \sqrt{2B_2}$	14.281	13.5605	10.719	10.539	7.9062	6.3223
-10	$B_1 > \sqrt{2B_2}$	2.0269	1.54919	1.6739	1.957	2.2648	2.3779
	$B_1 = \sqrt{2B_2}$	3.1623	3.14658	3.1009	3.0289	2.9361	2.8284

In Table 1, it is observed that, as long as tensile initial stress increases, the frequencies also increase whatever the scaling effect parameter is. It should be noted that the increment of frequencies in case 1 is much more than those in other two cases. When initial stress is compressive, the frequency parameters for clamped micro/nano beam with various scaling effect parameters are calculated for all cases and presented in Table 2.

Table 2. Frequency parameter for clamped micro/nano beam with various scaling effect and compressive initial stresses for all cases

	Case	Alpha(α)

Initial Stress		0	0.1	0.2	0.3	0.4	0.5
	$B_1 < \sqrt{2B_2}$	0	0	0	0	0	0
2	$B_1 > \sqrt{2B_2}$	1.5020	1.48324	1.249	1.1426	1.1189	1.0117
	$B_1 = \sqrt{2B_2}$	1.787	1.74893	1.6343	1.4394	1.149	0.6909
	$B_1 < \sqrt{2B_2}$	0	0	0	0	0	0
3	$B_1 > \sqrt{2B_2}$	1.4703	1.43652	1.3360	1.1897	1.0174	0.7071
	$B_1 = \sqrt{2B_2}$	1.481	1.4203	1.2287	0.8519	0	0
	$B_1 < \sqrt{2B_2}$	0	0	0	0	0	0
6	$B_1 > \sqrt{2B_2}$	1.4175	1.37369	1.2334	0.9592	0.9917	0.4987
	$B_1 = \sqrt{2B_2}$	0	0	0	0	0	0
	$B_1 < \sqrt{2B_2}$	0	0	0	0	0	0
8	$B_1 > \sqrt{2B_2}$	1.4147	1.35661	1.1662	0.7483	0.7483	0
	$B_1 = \sqrt{2B_2}$	0	0	0	0	0	0
	$B_1 < \sqrt{2B_2}$	0	0	0	0	0	0
10	$B_1 > \sqrt{2B_2}$	1.4143	1.34165	1.0955	0.4472	0	0
	$B_1 = \sqrt{2B_2}$	0	0	0	0	0	0
	$B_1 < \sqrt{2B_2}$	0	0	0	0	0	0
12	$B_1 > \sqrt{2B_2}$	1.4142	1.32665	1.0198	0.2009	0	0

	$B_1 = \sqrt{2B_2}$	0	0	0	0	0	0
	$B_1 < \sqrt{2B_2}$	0	0	0	0	0	0
14	$B_1 > \sqrt{2B_2}$	1.4142	1.31149	0.9381	0	0	0
	$B_1 = \sqrt{2B_2}$	0	0	0	0	0	0
	$B_1 < \sqrt{2B_2}$	0	0	0	0	0	0
16	$B_1 > \sqrt{2B_2}$	1.4142	1.29615	0.8485	0	0	0
	$B_1 = \sqrt{2B_2}$	0	0	0	0	0	0
	$B_1 < \sqrt{2B_2}$	0	0	0	0	0	0
18	$B_1 > \sqrt{2B_2}$	1.4142	0.83266	0.4968	0	0	0
	$B_1 = \sqrt{2B_2}$	0	0	0	0	0	0

In Table 2, it is seen that, the existence of compressive initial stress results in a reduction in frequencies whatever the scaling effect parameter is. For instance, in case 3, when $\Lambda = 8$ Pa, the frequencies become zero with $\alpha = 0.5$. If $\Lambda > 8$ Pa, the value of frequencies decrease and even become zero with $\alpha=0.3$ (if $\Lambda>13$ Pa) and 0.4, 0.5. However in case 2, $\Lambda = 3$ Pa, the frequencies become zero with $\alpha = 0.4$ and 0.5. Furthermore, the frequencies are all zero for case 1. In view of same numerical data, all three cases are considered and analyzed.

For case 1, frequency analysis of a clamped end micro/nano beams with initial stresses is performed by plotting frequencies for various scaling effect parameter (alpha) with both initial stresses such as tensile and compressive. It is presented in Figure 1. Variation of frequencies of the same beam for different tensile initial stresses is illustrated in Figure 2.
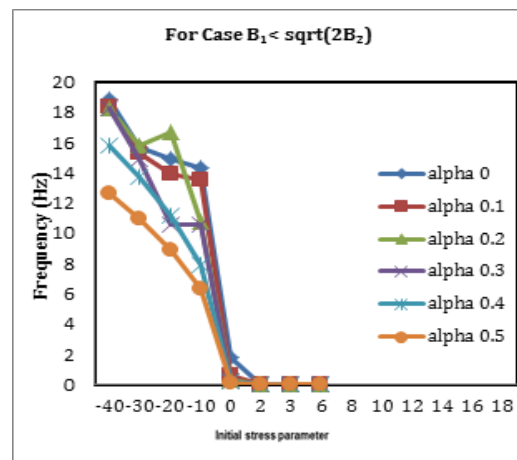

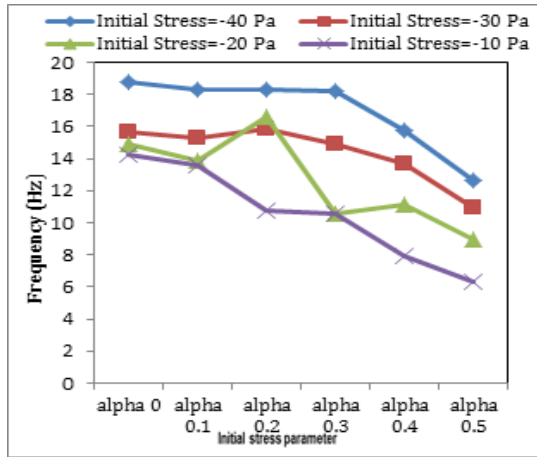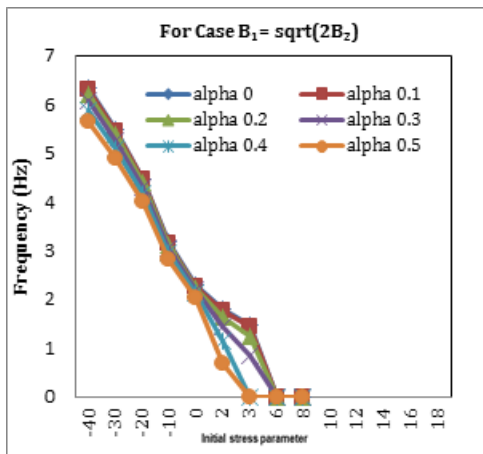**Figure 1.** Frequencies of clamped end micro/nano beams for different alpha values in case 1

Figure 2. Frequencies of clamped end micro/nano beams for different tensile initial stress in case 1

As shown in Figure 1 and 2, as the scaling effect parameter increased, the frequency decreased. Providing small scaling effect condition, higher tensile initial stresses increases the frequencies.

For case 2, frequency of a clamped end micro/nano beams with initial stresses is analyzed by plotting frequencies for various scaling effect parameter (alpha) with both initial stresses such as tensile and compressive. It is illustrated in Figure 3. Variation of frequencies of the same beam for different tensile initial stresses is shown in Figure 4. Moreover, variation of frequencies of the same beam for different compressive stresses is presented in Figure 5.

Figure 3. Frequencies of clamped end micro/nano beams for different alpha values in case 2
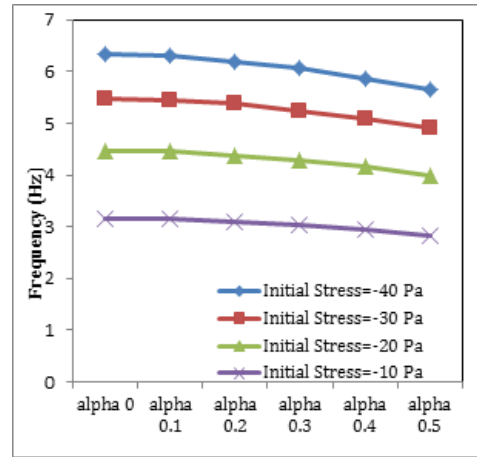

Figure 4. Frequencies of clamped end micro/nano beams for different tensile initial stress in case 2
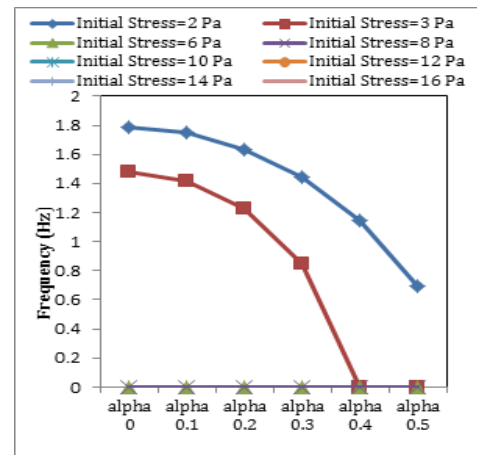

Figure 5. Frequencies of clamped end micro/nano beams for different compressive initial stress in case 2

To Figure 3, 4 and 5, as the scaling effect parameter increased, the frequency decreased. The frequency values are close to each other for different scaling effect in Figure 3. Providing small scaling effect condition, higher tensile initial stresses increases the frequencies in Figure 4. However, if the case is the presence of compressive initial stress, frequencies decrease as compressive initial stress increase in also larger scaling effect. When $\Lambda \geq 6$ Pa, the frequencies are all zero.

For case 3, frequency of a clamped end micro/nano beams with initial stresses is presented by plotting frequencies for various scaling effect parameter (alpha) with both initial stresses such as tensile and compressive. It is shown in Figure 6. Variation of frequencies of the same beam for different tensile initial stresses is presented in Figure 7. Besides,

variation of frequencies of the same beam for different compressive stresses is illustrated in Figure 8.
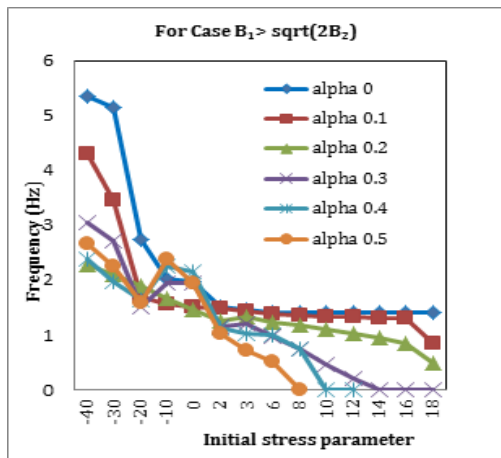

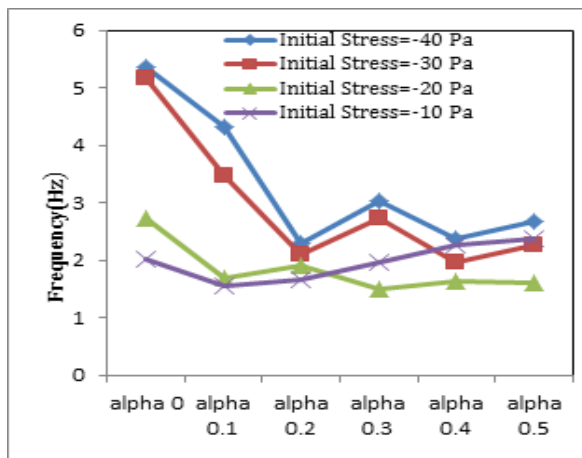**Figure 6.** Frequencies of clamped end micro/nano beams for different alpha values in case 3

Figure 7. Frequencies of clamped end micro/nano beams for different tensile initial stress in case 3
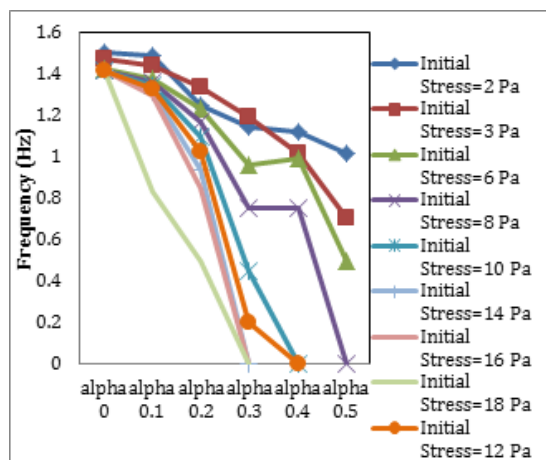

Figure 8. Frequencies of clamped end micro/nano beams

for different compressive initial stress in case 3

As shown in Figure 6, 7 and 8, as the scaling effect parameter increased, the frequency decreased. Providing small scaling effect condition, higher tensile initial stresses increases the frequencies in Figure 7.

Besides, if the case is the presence of compressive initial stress, frequencies decrease as compressive initial stress increase in also larger scaling effect. When $\Lambda \geq 8$ Pa, the frequencies become zero in larger scaling effects such as 0.4 and 0.5 in Figure 8.

4 Discussion and Conclusions

Eringen's nonlocal elasticity and nonlocal Euler–Bernoulli theories are developed, and exact solutions are obtained for vibration of initially stressed clamped end micro/nano beam. This paper propounds a developed approach for attaining frequencies of micro/nano beam with the consideration of the presence of initial stress by employing the constituted finite element.

Exact dynamic shape functions and stiffness terms for each case are obtained and presented explicitly by also use of Hamiltonian's principle for the governing equations.

The following observations and results are attained from the figures and tables:

1) For all cases, the effect of tensile stress increases frequencies whereas compressive initial stress results in a decrease in frequencies.

2) For cases 2 and 3, the frequency value leads to a decrease with an increase in compressive initial stress until it is zero when the critical buckling stress is reached. For case 2, it is seen in Figure 5 that, critical buckling stress is 3 Pa. While for case 3, the critical buckling stress is 8 Pa which is observed in Figure 8.

3) The allowance for the small scale effect leads to increase in frequencies for all cases.

4) At the limiting situations of the physical parameters (such as, $\alpha \rightarrow 0$, $\Lambda \rightarrow 0$ and $\lambda \rightarrow 0$), the derived shape functions converge to the Hermitian shape functions.

5) This finite element formulation take accounts of the effects of initial stress, small length scale, which become important in micro/nano beams, especially for short and stubby beams and as the frequencies are high.

6) The method is also practicable for acquiring the bending and buckling solutions of with initially stressed micro/nano beams using the nonlocal beam theory based on Euler-Bernoulli beam theory.

7) This method results in minimal computational

effort with the benefit of using only one element. Moreover, the present work can be furthered to analysis and design of nanostructures with complicated geometries and different load conditions under different boundary conditions and also higher order beam theories for precise analysis of thick nanostructures

6 References

[1] Iijima, S. Nanotubes. Nature. 1999; 354, 56-58.

[2] Mongillo, J. Nanotechnology 101; Press: Greenwood, London, 2009; 299 pp.

[3] Wilson, M.; Kannangara K.; Smith, G.; Simmons, M.; Raguse, B.; Nanotechnology, Basic Science and Emerging Technologies. Press: Chapman&Hall/CRC, Australia, 2002; 290 pp.

[4] Wang, L.F.; Hu, H.Y. Flexural wave propagation in single-walled carbon nanotubes. Phys. Rev. B. 2005; 71, 195412.

[5] Eringen, A.C. Nonlocal polar elastic continua. Int. J. Eng. Sci. 1972; 10, 1-16.

[6] Eringen, A.C.; Edelen, D. On nonlocal elasticity. Int. J. Eng. Sci. 1972; 10, 233-248.

[7] Eringen, A.C. On differential equations of nonlocal elasticity and solutions of screw dislocation and surface waves. J. Appl. Phys. 1983; 54, 4703-4710.

[8] Peddieson, J.; Buchanan, G.R.; McNitt, R.P. Application of nonlocal continuum models to nanotechnology. Int. J. Eng. Sci. 2003; 41, 305-312.

[9] Sudak, L.J. Column buckling of multiwalled carbon nanotubes using nonlocal continuum mechanics. J. Appl. Phys. 2003; 94, 7281-7287.

[10] Zhang; Y.Q.; Liu, G.R.; Xie, X.Y. Transverse vibrations of double-walled carbon nanotubes using a theory of nonlocal elasticity. Phys. Lett. A. 2005; 340, 258-266.

[11] Wang, Q. Wave propagation in carbon nanotubes via nonlocal continuum mechanics. J. Appl. Phys. 2005; 98, 124301-124306.

[12] Wang, Q.; Varadan, V.K. Vibration of carbon nanotubes studied using nonlocal continuum mechanics. Smart. Mater. Struct. 2006; 15, 659-666.

[13] Lu, P.; Lee, H.P.; Lu, C.; Zhang, P.Q.; Dynamic properties of flexural beams using a nonlocal elasticity model. J. Appl. Phys. 2006; 99, 073510.

[14] Xu, M. Free transverse vibrations of nano-to-micron scale beams. Proceedings of the Royal Society A. 2006; 462, 2977-2995.

[15] Wang, C.M.; Zhang, Y.Y.; He, X.Q. Vibration of nonlocal Timoshenko beams. Nanotechnology, 2007; 18, 105401-105410.

[16] Lee, Y.Y.; Wang, C.M.; Kitipornchai, S. Vibration of Timoshenko beam with internal hinge. J. Eng. Mech. 2003; 129, 293–301.

[17] Timoshenko, S.P. Vibration Problems in Engineering. Press: Wiley, New York, 1974; 624 pp.

[18] Prasad, P. On the response of a Timoshenko beam under initial stress to a moving load. Int. J. Eng. Sci. 1981; 19, 615-628.

[19] Shames, I.H., Dym, C.L. Energy and Finite Element Methods in Structural Mechanics. Press: Mc-Graw-Hill, New York, 1985; 776 pp.

[20] Yoon, J.; Ru, C.Q.; Mioduchowski, A. Timoshenko-beam effects on transverse wave propagation in carbon nanotubes. Compos. Part B-Eng. 2004; 35, 87-93.

[21] Koh, S.J.A.; Lee, H.P. Molecular dynamics simulation of size and strain rate dependent mechanical response of FCC metallic nanowires. Nanotechnology. 2006; 17, 3451–3467.

[22] Wang, C.M.; Zhang, Y.Y.; Kitipornchai, S. Vibration of initially stressed micro- and nano-beams. International Journal of Structural Stability and Dynamics. 2007; 7, 555-570.

[23] Phadikar, J.K.; Pradhan, S.C. Variational formulation and finite element analysis for nonlocal elastic nanobeams and nanoplates. Comp. Mater. Sci. 2010; 49, 492-499.

[24] Pradhan, S.C. Nonlocal finite element analysis and small scale effects of CNTs with Timoshenko beam theory. Finite Elem. Anal. Des. 2012; 50, 8-20.

[25] Adhikari, S.; Murmu, T.; McCarthy, M.A. Dynamic finite element analysis of axially vibrating nonlocal rods. Finite Elem. Anal. Des. 2013; 63, 42-50.

[26] Cook, R.D.; Malkus, D.S.; Plesha, M.E.; Witt, R.J. Concepts and Applications of Finite Element Analysis. Press: John Wiley&Sons, New York, 2001; 736 pp.

[27] Franklin, Y.C. Matrix Analysis of Structural Dynamics, Applications and Earthquake Engineering. Press: Marcel Dekker, Inc., New York, 2001; 989 pp.

[28] Alemdar, B.N; Gülkan, P. Beams on generalized foundations: supplementary element matrices. Eng. Struct. 1997; 19, 910-920.

[29] Dinçkal, Ç. Free vibration analysis of Carbon Nanotubes by using finite element method. Iran. J. Sci. Technol. Trans. Mech. Eng. 2016; 40, 43-55.

[30] Dinçkal, Ç.; Alemdar, B.N.; Gülkan, P.H. Dynamics of a beam-column element on an elastic foundation. Can. J. Civ. Eng. 2016; 43, 685-701.

[31] Wolfram, S. Mathematica: A System For Doing Mathematics By Computer. Press: Addison-Wesley, Redwood City, California, 1988; 961 pp.

Appendix A

$$N_1 = \frac{\begin{array}{c}(\xi^2\cos[\xi x])\cosh[\eta(2L-x)]+\\ \eta^2\cos[\xi(2L-x)]\cosh[\eta x]-\\ \xi^2\cos[\xi x]\cosh[\eta x]-\eta^2\cos[\xi x]\cosh[\eta x]+\\ \xi\eta\sin[\xi x]\sinh[\eta(2L-x)]-\\ \xi\eta\sin[\xi(2L-x)]\sinh[\eta x])\end{array}}{(-\xi^2-\eta^2+\eta^2\cos[2L\xi]+\xi^2\cosh[2\eta L])} \quad (A1)$$

$$N_2 = \frac{\begin{array}{c}(\xi\cosh[\eta(2L-x)]\sin[\xi x]-\xi\cosh[\eta x]\sin[\xi x]+\\ \eta\cos[\xi(2L-x)]\sinh[\eta x]-\eta\cos[\xi x]\sinh[\eta x])\end{array}}{(-\xi^2-\eta^2+\eta^2\cos[2L\xi]+\xi^2\cosh[2\eta L])} \quad (A2)$$

$$N_3 = \frac{\begin{pmatrix}\xi^2\cos[\xi(L-x)]\cosh[\eta(L-x)]+\\ \eta^2\cos[\xi(L-x)]\cosh[\eta(L-x)]-\\ \eta^2\cos[\xi(L+x)]\cosh[\eta(L-x)]\\ -\xi^2\cos[\xi(L-x)]\cosh[\eta(L+x)]+c\end{pmatrix}}{(\xi^2+\eta^2-\eta^2\cos[2L\xi]+\xi^2\cosh[2\eta L])} \quad (A3)$$

where

$$c = \xi\eta\sin[\xi(L+x)]\sinh[\eta(L-x)] - \xi\eta\sin[\xi(L-x)]\sinh[\eta(L+x)] \quad (A4)$$

$$N_4 = \frac{\begin{array}{c}(-(\xi\cosh[\eta(L-x)]\sin[\xi(L-x)])+\\ \xi\sin[\xi(L-x)]\cosh[\eta(L+x)]-\\ \eta\cos[\xi(L-x)]\sinh[\eta(L-x)]+\\ \eta\cos[\xi(L+x)]\sinh[\eta(L-x)])\end{array}}{(\xi^2+\eta^2-\eta^2\cos[2L\xi]+\xi^2\cosh[2\eta L])} \quad (A5)$$

Appendix B

$$N_1 = \frac{\begin{array}{c}(\cos[(2L-x)\beta]-\cos[\beta x]+2L^2\beta^2\cos[x\beta]-2Lx\beta^2\cos[x\beta]-\\ x\beta\sin[(2L-x)\beta]+2L\beta\sin[x\beta]-x\beta\sin[x\beta])\end{array}}{(-1+2L^2\beta^2+\cos[2L\beta])} \quad (B1)$$

$$N_2 = \frac{(x\cos[(2L-x)\beta]-x\cos[x\beta]+2L^2\beta\sin[x\beta]-2Lx\beta\sin[x\beta])}{(-1+2L^2\beta^2+\cos[2L\beta])} \quad (B2)$$

$$N_3 = \frac{\begin{array}{c}(-\cos[(L-x)\beta]+2Lx\beta^2\cos[(L-x)\beta]+\cos[(L+x)\beta]+\\ L\beta\sin[(L-x)\beta]+x\beta\sin[(L-x)\beta]-L\beta\sin[(L+x)\beta]+\\ x\beta\sin[(L+x)\beta])\end{array}}{(-1+2L^2\beta^2+\cos[2L\beta])} \quad (B3)$$

$$N_4 = \frac{\begin{array}{c}(-L\cos[(L-x)\beta]+x\cos[(L-x)\beta]+L\cos[(L+x)\beta]-\\ x\cos[(L+x)\beta]+2Lx\beta\sin[(L-x)\beta])\end{array}}{(1-2L^2\beta^2-\cos[2L\beta])} \quad (B4)$$

Appendix C

$$N_1 = \frac{\begin{array}{c}(-(\gamma^2\cos[(\gamma-\beta)x])+\beta^2\cos[(\gamma-\beta)x]-\gamma^2\cos[(\gamma+\beta)x]+\\ \beta^2\cos[(\gamma+\beta)x]+\\ \gamma\beta\cos[2\gamma L-\gamma x-\beta x]-\beta^2\cos[2\gamma L-\gamma x-\beta x]+d)\end{array}}{(2(-\gamma^2+\beta^2-\beta^2\cos[2L\gamma]+\gamma^2\cos[2\beta L]))} \quad (C1)$$

where

$$d = \gamma^2\cos[2\beta L-\gamma x-\beta x] - \gamma\beta\cos[2\beta L-\gamma x-\beta x] + (\gamma^2+\gamma\beta)\cos[2\beta L+\gamma x-\beta x] -$$

$$\gamma\beta\cos[2\gamma L-\gamma x+\beta x] - \beta^2\cos[2\gamma L-\gamma x+\beta x] \quad (C2)$$

$$N_2 = \frac{\begin{array}{c}((\gamma\sin[(\gamma-\beta)x])+\beta\sin[(\gamma-\beta)x]+\gamma\sin[(\gamma+\beta)x]\\ -\beta\sin[(\gamma+\beta)x]\\ -\beta\sin[2\gamma L-\gamma x-\beta x]\\ +\gamma\sin[2\beta L-\gamma x-\beta x]]\\ -\gamma\sin[2\beta L+\gamma x-\beta x]+\beta\sin[2\gamma L-\gamma x+\beta x])\end{array}}{(2(\gamma^2-\beta^2+\beta^2\cos[2L\gamma]-\gamma^2\cos[2\beta L]))} \quad (C3)$$

$$N_3 = \frac{\begin{array}{c}(-(\gamma^2\cos[(\gamma+\beta)(L-x)])+\beta^2\cos[(\gamma+\beta)(L-x)]+\\ \gamma^2\cos[(\gamma L-\beta L)-(\gamma x+\beta x)]\\ -\gamma\beta\cos[\gamma L-\gamma x-\beta x-\beta L]+e)\end{array}}{(2(-\gamma^2+\beta^2-\beta^2\cos[2*L*\gamma]+\gamma^2\cos[2*\beta*L]))} \quad (C4)$$

Where

$$e = (-\gamma\beta-\beta^2)\cos[\gamma L+\beta L+\gamma x-\beta x] +$$

$$(-\gamma^2+\beta^2)\cos[\gamma L-\beta L-\gamma x+\beta x] +$$

$$(\gamma^2+\gamma\beta)\cos[\gamma L+\beta L-\gamma x+\beta x] + (\gamma\beta-\beta^2)\cos[\gamma L-\beta L+\gamma x+\beta x] \quad (C5)$$

$$N_4 = \frac{\begin{array}{c}(\gamma\sin[(\gamma+\beta)(L-x)]-\beta\sin[(\gamma+\beta)(L-x)]-\\ \gamma\sin[\gamma L-\beta L-\gamma x-\beta x]+f)\end{array}}{(2(-\gamma^2+\beta^2-\beta^2\cos[2L\gamma]+\gamma^2\cos[2\beta L]))} \quad (C6)$$

$$f = \beta\sin[\gamma L+\beta L+\gamma x-\beta x] + \gamma\sin[\gamma L-\beta L-\gamma x+\beta x] + \beta\sin[\gamma L-\beta L-\gamma x+\beta x] - \gamma\sin[\gamma L+\beta L-\gamma x+\beta x] - \beta\sin[\gamma L-\beta L+\gamma x+\beta x] \quad (C7)$$

Appendix D

$$k_{11} = \frac{2\,EI\,\xi\,\eta\,(\xi^2+\eta^2)\,(\eta\,\sin[2L\xi]+\xi\,\sinh[2L\eta\,])}{-\xi^2-\eta^2+\eta^2\cos[2L\xi]+\xi^2\cosh[2L\eta]} \quad (D1)$$

$$k_{12} = \frac{EI\,(\xi^2+\eta^2)\,(-\xi^2+\eta^2-\eta^2\cos[2L\xi]+\xi^2\cosh[2L\eta])}{-\xi^2-\eta^2+\eta^2\cos[2L\xi]+\xi^2\cosh[2L\eta]} \quad (D2)$$

$$k_{13} = \frac{4\,EI\,\xi\,\eta\,(\xi^2+\eta^2)\,(\eta\,\cosh[L\eta]\sin[L\xi]+\xi\,\cos[L\xi]\sinh[L\eta])}{\xi^2+\eta^2-\eta^2\cos[2L\xi]-\xi^2\cosh[2L\eta]}$$
$$(D3)$$

$$k_{14} = \frac{4\,EI\,\xi\,\eta\,(\xi^2+\eta^2)\,\sin[L\xi]\sinh[L\eta]}{-\xi^2-\eta^2+\eta^2\cos[2L\xi]+\xi^2\cosh[2L\eta]} \quad (D4)$$

$$k_{22} = \frac{2\,EI\,\xi\,\eta\,(-\eta\,\sin[2\,L\,\xi]+\xi\,\sinh[2\,L\,\eta\,])}{-\xi^2-\eta^2+\eta^2\cos[2L\xi]+\xi^2\cosh[2L\eta]} \quad (D5)$$

$$k_{23} = \frac{4\,EI\,\xi\,\eta\,(\xi^2+\eta^2)\,\sin[L\xi]\sinh[L\eta]}{-\xi^2-\eta^2+\eta^2\cos[2L\xi]+\xi^2\cosh[2L\eta]} \quad (D6)$$

$$k_{24} = \frac{4\,EI\,\xi\,\eta\,(-\eta\,\cosh[L\,\eta]\,\sin[L\xi]+\xi\,\cos[L\,\xi]\sinh[L\eta\,])}{\xi^2+\eta^2-\eta^2\cos[2L\xi]-\xi^2\cosh[2L\eta]} \quad (D7)$$

$$k_{33} = k_{11}, \qquad k_{34} = -k_{12}, \qquad k_{44} = k_{22}$$
$$(D8)$$

Appendix E

$$k_{11} = \frac{2\,EI\,\beta^3\,(2\,L\beta+\sin[2L\beta])}{-1+2\,L^2\,\beta^2+\cos[2L\beta]} \quad (E1)$$

$$k_{12} = \frac{EI\,\beta^2\,(1+2\,L^2\,\beta^2-\cos[2L\beta\,])}{-1+2\,L^2\,\beta^2+\cos[2L\beta]} \quad (E2)$$

$$k_{13} = -\frac{4\,EI\,\beta^3\,(L\,\beta\,\cos[L\beta]+\sin[L\beta])}{-1+2\,L^2\,\beta^2+\cos[2L\beta]} \quad (E3)$$

$$k_{14} = \frac{4\,EI\,L\,\beta^3\,\sin[L\beta]}{-1+2\,L^2\,\beta^2+\cos[2L\beta]} \quad (E4)$$

$$k_{22} = \frac{2\,EI\,\beta\,(2\,L\beta-\sin[2L\beta])}{-1+2\,L^2\,\beta^2+\cos[2L\beta]} \quad (E5)$$

$$k_{23} = \frac{4\,EI\,L\,\beta^3\,\sin[L\beta]}{-1+2\,L^2\,\beta^2+\cos[2L\beta]} \quad (E6)$$

$$k_{24} = -\frac{4\,EI\,\beta\,(L\,\beta\,\cos[L\beta]-\sin[L\beta\,])}{-1+2\,L^2\,\beta^2+\cos[2L\beta]} \quad (E7)$$

$$k_{33} = k_{11}, \qquad k_{34} = -k_{12}, \qquad k_{44} = k_{22} \quad (E8)$$

Appendix F

$$k_{11} = -\frac{EI\,\beta\,(\beta-\gamma)\,\gamma\,(\beta+\gamma)\,(\beta\,\cos[L\gamma]\sin[L\beta]-\gamma\,\cos[L\beta]\sin[L\gamma])}{2\beta\gamma\,(-1+\cos[L\beta]\cos[L\gamma])+(\beta^2+\gamma^2)\,\sin[L\beta]\sin[L\gamma]}$$
$$(F1)$$

$$k_{12} =$$
$$\frac{EI\,\beta\,\gamma\,\big((\beta^2+\gamma^2)\,(-1+\cos[L\beta]\cos[L\gamma])+2\beta\gamma\,\sin[L\beta]\sin[L\gamma]\big)}{2\beta\gamma\,(-1+\cos[L\beta]\cos[L\gamma])+(\beta^2+\gamma^2)\sin[L\beta]\sin[L\gamma]} \quad (F2)$$

$$k_{13} = \frac{EI\,\beta\,(\beta-\gamma)\,\gamma\,(\beta+\gamma)\,(\beta\,\sin[L\beta]-\gamma\,\sin[L\gamma])}{2\beta\gamma\,(-1+\cos[L\beta]\cos[L\gamma])+(\beta^2+\gamma^2)\,\sin[L\beta]\sin[L\gamma]} \quad (F3)$$

$$k_{14} = \frac{EI\,\beta\,(\beta-\gamma)\,\gamma\,(\beta+\gamma)\,(\cos[L\beta]-\cos[L\gamma])}{2\beta\gamma\,(-1+\cos[L\beta]\cos[L\gamma])+(\beta^2+\gamma^2)\,\sin[L\beta]\sin[L\gamma]} \quad (F4)$$

$$k_{22} = \frac{EI\,(\beta-\gamma)\,(\beta+\gamma)(-\gamma\,\cos[L\gamma]\sin[L\beta]+\beta\cos[L\beta]\sin[L\gamma])}{2\beta\gamma\,(-1+\cos[L\beta]\cos[L\gamma])+(\beta^2+\gamma^2)\,\sin[L\beta]\sin[L\gamma]}$$
$$(F5)$$

$$k_{23} = -\frac{EI\,\beta\,(\beta-\gamma)\,\gamma\,(\beta+\gamma)(\cos[L\beta]-\cos[L\gamma])}{2\beta\gamma\,(-1+\cos[L\beta]\cos[L\gamma])+(\beta^2+\gamma^2)\,\sin[L\beta]\sin[L\gamma]}$$
$$(F6)$$

$$k_{24} = -\frac{EI\,(\beta-\gamma)\,(\beta+\gamma)(-\gamma\,\sin[L\beta]+\beta\,\sin[L\gamma])}{2\beta\gamma\,(-1+\cos[L\beta]\cos[L\gamma])+(\beta^2+\gamma^2)\,\sin[L\beta]\sin[L\gamma]}$$
$$(F7)$$

$$k_{33} = k_{11}, \qquad k_{34} = -k_{12}, \qquad k_{44} = k_{22}$$
$$(F8)$$